Human Molecular Genetics, 2016, Vol. 25, No. 12 2552–2563

doi: 10.1093/hmg/ddw118
Advance Access Publication Date: 22 April 2016
Original Article

ORIGINAL ARTICLE

In vitro and *in vivo* rescue of aberrant splicing in *CEP290*-associated LCA by antisense oligonucleotide delivery

Alejandro Garanto[1,2], Daniel C. Chung[3], Lonneke Duijkers[1], Julio C. Corral-Serrano[1,4], Muriël Messchaert[1,2], Ru Xiao[5], Jean Bennett[3], Luk H. Vandenberghe[5] and Rob W.J. Collin[1,2,*]

[1]Department of Human Genetics, [2]Donders Center for Neurosciences, Radboud University Medical Center, 6525 GA Nijmegen, The Netherlands, [3]F.M. Kirby Center for Molecular Ophthalmology and Center for Advanced Retinal and Ophthalmic Therapeutics, Scheie Eye Institute, University of Pennsylvania School of Medicine, Philadelphia, PA 19104, USA, [4]Radboud Institute for Molecular Life Sciences, Radboud University Medical Center, 6525 GA Nijmegen, The Netherlands and [5]Grousbeck Gene Therapy Center, Department of Ophthalmology, Schepens Eye Research Institute, Massachusetts Eye and Ear Infirmary, Harvard Medical School, Boston, MA 02114, USA

*To whom correspondence should be addressed: Rob W.J. Collin, PhD, Department of Human Genetics (855), Radboud, University Medical Center Geert Grooteplein Zuid 10, 6525 GA Nijmegen, The Netherlands. Tel: +31 24 3613750; Fax: +31 24 3668752; E-mail: rob.collin@radboudumc.nl

Abstract

Leber congenital amaurosis (LCA) is a severe disorder resulting in visual impairment usually starting in the first year of life. The most frequent genetic cause of LCA is an intronic mutation in *CEP290* (c.2991 + 1655A > G) that creates a cryptic splice donor site resulting in the insertion of a pseudoexon (exon X) into *CEP290* mRNA. Previously, we showed that naked antisense oligonucleotides (AONs) effectively restored normal *CEP290* splicing in patient-derived lymphoblastoid cells. We here explore the therapeutic potential of naked and adeno-associated virus (AAV)-packaged AONs *in vitro* and *in vivo*. In both cases, AON delivery fully restored *CEP290* pre-mRNA splicing, significantly increased CEP290 protein levels and rescued a ciliary phenotype present in patient-derived fibroblast cells. Moreover, administration of naked and AAV-packaged AONs to the retina of a humanized mutant *Cep290* mouse model, carrying the intronic mutation, showed a statistically significant reduction of exon X-containing *Cep290* transcripts, without compromising the retinal structure. Together, our data highlight the tremendous therapeutic prospective of AONs for the treatment of not only *CEP290*-associated LCA but potentially many other subtypes of retinal dystrophy caused by splicing mutations.

Introduction

Leber congenital amaurosis (LCA; OMIM 204000) is the most severe subtype of inherited retinal dystrophy (IRD) with a prevalence of ∼1:50 000 in the European and North-American populations (1,2). The clinical characteristics of LCA are severe and early loss of vision, amaurotic pupils, sensory nystagmus and the absence of electrical signals on electroretinogram (3).

Received: March 3, 2016. **Revised:** April 8, 2016. **Accepted:** April 12, 2016

LCA shows a high genetic heterogeneity and to date, mutations in 23 different genes have been associated with LCA (RetNet: https://sph.uth.edu/retnet, last accessed April 23, 2016), mainly segregating in an autosomal recessive manner. The gene most frequently mutated in LCA is *CEP290* (centrosomal protein 290 kDa) (3–5), a gene that encompasses 54 exons and encodes a 2479 amino acid protein (6) localized in the centrosome and in the basal body of cilia (7). Of all *CEP290* mutations that cause non-syndromic LCA, a deep-intronic variant (c. 2991 + 1655A > G) is by far the most recurrent one, accounting for up to 15% of LCA cases in many Western countries (5,8–10). This mutation creates a cryptic splice donor site, resulting in the insertion of an aberrant pseudoexon (exon X) with a premature stop codon into ∼50% of all *CEP290* transcripts (5).

For many years, IRDs have been considered incurable diseases. However, in the last decade major progress has been accomplished in different therapeutic areas, such as retinal prosthesis, cell transplantation and gene therapy. Phase I/II clinical trials using gene augmentation therapy have shown to be safe and moderately effective in LCA and early-onset IRD patients with mutations in *RPE65* (11–15), and in choroideremia patients with a mutation in *CHM* (16). In these studies, the wild-type cDNA of *RPE65* and *CHM*, respectively, was packaged in replication-defective recombinant adeno-associated viruses (AAVs) and delivered to the retina by a single surgical procedure. The restricted cargo size of AAVs (∼5 kb) however has so far hampered a fast and broad implementation of AAV-based gene augmentation therapy for several other genetic subtypes of IRD, since the cDNA size of many genes that cause IRD, including that of *CEP290*, exceed the cargo limit of AAVs.

One alternative strategy to treat *CEP290*-associated LCA utilizes antisense oligonucleotides (AONs), small RNA molecules that bind to their target mRNA in a complementary fashion and subsequently can interfere with pre-mRNA splicing. AONs have already been shown to be effective therapeutic molecules in several inherited disorders *in vitro* (17) and are currently being used in clinical trials for Duchenne's muscular dystrophy (18,19), several cancer types (20,21), familial hypercholesterolemia (22), viral infections and neovascular disorders (23) amongst others. The intronic *CEP290* mutation is an ideal target for AON-based therapy, as skipping the pseudoexon that is inserted to the *CEP290* mRNA as a result of the c.2991 + 1655A > G change, would fully restore normal *CEP290* splicing and wild-type CEP290 protein levels. Recently, we and others have shown that transfection of naked AON molecules indeed restores normal *CEP290* splicing in cultured cells of LCA patients with homozygous intronic *CEP290* mutations (24,25). In future trials however, administrating AONs to the retina of patients with *CEP290*-associated LCA would require multiple injections of naked AONs, as the stability of these molecules amongst others depends on chemical modifications and target cell or tissue, and ranges from hours to months (23,26). An alternative way of delivering AONs would be to use AAVs, as a single subretinal injection of AAVs could give rise to a persistent expression in the retina, as shown in dog and primate models (27,28). Hence, we here compare the therapeutic efficacy of naked AONs as well as those cloned into AAVs, both *in vitro* and *in vivo*, and provide evidence that both delivery methods are promising approaches for the development of a splice correction therapy for *CEP290*-associated LCA.

Results

In this study, we aimed to explore the therapeutic efficacy of AONs, to correct a splice defect resulting from a recurrent intronic mutation in *CEP290* both *in vitro* and *in vivo*, using naked molecules and AON-containing AAVs. Previously, we showed that delivery of naked AON molecules (modified with a 2′-O-methyl group and a phosphorothioate backbone) restores normal *CEP290* splicing in lymphoblastoid cells from LCA patients homozygously carrying the intronic *CEP290* mutation (24). To determine the consequences of splice correction at the protein and cellular level, fibroblast cell lines were generated from LCA patients with the intronic *CEP290* mutation, as these fibroblasts, unlike lymphoblastoid cells, endogenously express the CEP290 protein and develop cilia when cultured under serum starved conditions. Similar to what was observed in lymphoblasts (24), transfection of naked AONs to the patient's fibroblast cells completely restored normal *CEP290* splicing, with a minimal effective concentration of 0.05 μmol/l (data not shown). For all *in vitro* experiments we used the naked AON reported as AON3 in our previously published work (24) at a final concentration of 0.1 μmol/l.

In order to deliver AONs in an adeno-associated viral context, a modified U7snRNA construct was used. This allows the synthesis of the RNA molecules and an effective delivery of AONs to the right nuclear compartment for splicing intervention (29). Different AON sequences (or combinations thereof) were cloned into the pSMD2 vector that contains the modified mouse U7snRNA as well as inverted terminal repeat (ITR) sequences (29) needed for AAV generation (Fig. 1A), yielding six different constructs with AONs (pAAV-AON1 to pAAV-AON6), as well as a construct without any AON that served as a negative control (pAAV-NoAON). However, upon transfection of these constructs into the patient's fibroblasts, no decrease in the amount of aberrantly spliced *CEP290* transcript was observed, due to the very low transfection efficiency in this cell type (data not shown). In order to assess the potential therapeutic efficacy of the generated constructs, two *CEP290* minigene constructs were generated that contained ∼6.4 kb of the human *CEP290* gene, including exon 26, the complete intron 26 (with and without the intronic mutation), and exon 27, flanked by two exons of the *RHO* gene (Fig. 1B). Transfection of these constructs in human embryonic kidney (HEK293T) cells revealed that the proportion of aberrantly versus correctly spliced *CEP290* transcripts was comparable to that observed in LCA fibroblast cells (Fig. 1C), hence mimicking the molecular consequences of the intronic *CEP290* mutation in these cells. Subsequent co-transfection of the *CEP290* minigene construct with the six different pAAV-AON constructs into HEK293T cells revealed that all constructs were able to redirect normal *CEP290* splicing, although not all as effectively as the naked AON (Fig. 2). To identify the most potent vectors, decreasing quantities of pAAV-AON constructs were transfected, revealing pAAV-AON4 and pAAV-AON5 as the most effective ones, as these were still able to fully restore *CEP290* splicing at the lowest concentration tested (Fig. 2). Thus, pAAV-AON4 and pAAV-AON5 constructs were selected for the generation of AAVs, together with the pAAV-NoAON construct.

The AAV capsid serotype determines the capability to infect certain cells or tissues. To determine which serotype was most suitable for our experiments, we transduced six different AAV serotypes carrying the cDNA of the Green fluorescent protein (GFP) under control of a cytomegalovirus (CMV) promoter. AAV2/2 showed the highest transduction efficiency, already at a multiplicity of infection (MOI) of 100, in both control and LCA patient fibroblast cells (Supplementary Material, Fig. S1A and B). Higher MOIs determined that AAV2/9 was also able to infect LCA patient fibroblast cells (Supplementary Material, Fig. S1C),

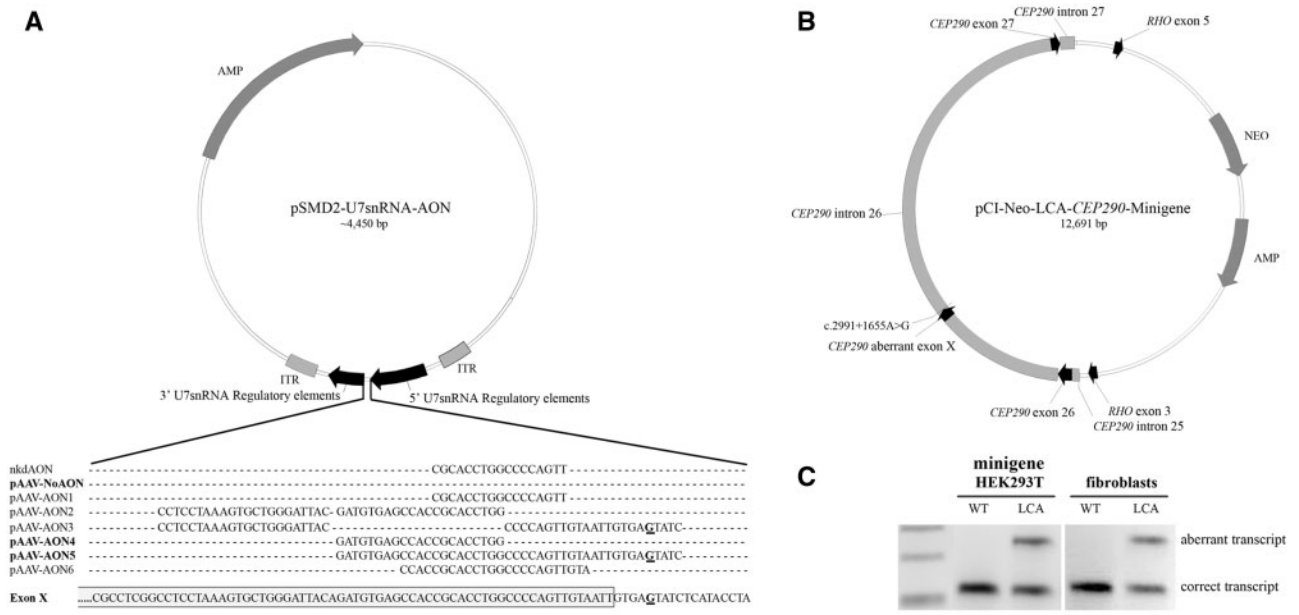

Figure 1. Generated constructs and assessment of minigenes. (**A**) Upper panel: graphical representation of the pSMD2 constructs containing the modified U7snRNA gene and inserted AON sequences. Lower panel: exact sequences of the AONs used in the different constructs, aligned with the sequence of the cryptic exon. The intronic c.2991 + 1655A>G mutation is indicated in bold and underlined. (**B**) Schematic drawing of the LCA minigene construct, containing the genomic DNA sequence of *CEP290* from intron 25 to intron 27, including the c.2991 + 1655A>G mutation in intron 26. This sequence is flanked by exon 3 and 5 of the *RHO* gene. (**C**) RT-PCR analysis of *CEP290* on HEK293T cells transfected with the WT or LCA minigene, in comparison with that in fibroblast cells from healthy controls or patients with *CEP290*-associated LCA.

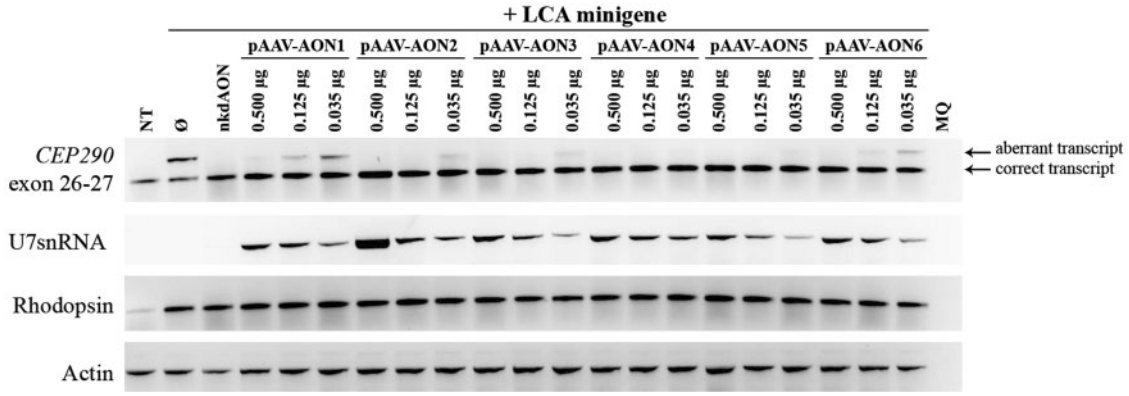

Figure 2. Splice correction efficacy of AON-containing vectors. HEK293T cells were co-transfected with the LCA minigene and three different concentrations of the six different pAAV-AON constructs (0.5, 0.125 or 0.035 µg of plasmid DNA). RT-PCR analysis from exon 26 to exon 27 of *CEP290* revealed the aberrant transcript that contains the cryptic exon X. pAAV-AON4 and pAAV-AON5 were most effective. Naked AON (nkdAON) was used as a positive control. U7snRNA and *RHO* amplification were used as a transfection control for the pAAV-AON and the minigene constructs, respectively. Actin was used as a loading control and MQ as the negative control of the PCR reaction. NT refers to non-transfected cells.

but AAV2/2 was selected for the generation of the AON-containing AAVs.

Following the generation of the three AAVs (i.e. AAV-NoAON, AAV-AON4 and AAV-AON5), the fibroblast cell lines of two unrelated LCA patients homozygously carrying the intronic *CEP290* mutation (LCA1 and LCA2) were transduced with these AAVs, at three different MOI, or transfected with the naked AON. RT-PCR analysis revealed that transduction of the two AON-containing AAVs almost completely restored normal *CEP290* splicing, with the highest efficacy observed at an MOI of 10 000, to a similar degree as the naked AON molecule (Fig. 3). In contrast, AAV-NoAON showed the same pattern as the untransduced cells, indicating that the rescue of aberrant *CEP290* splicing was caused by the actual AON sequences. Transduction of two control fibroblast cell lines (C1 and C2) with the different AAVs did not show any difference in the levels of expression of *CEP290* mRNA after transduction or transfection (Supplementary Material, Fig. S2A).

Next, we assessed whether restoring normal *CEP290* splicing resulted in an increase of wild-type CEP290 protein levels. Patient and control fibroblast cells were transduced with the three AAVs at a MOI of 10 000, or transfected with the naked AONs. Protein lysates were subjected to western blot analysis, using α-tubulin as a loading control. Although in the untreated fibroblast cells from the LCA patients, CEP290 protein levels were markedly reduced, cells transfected with the naked AON,

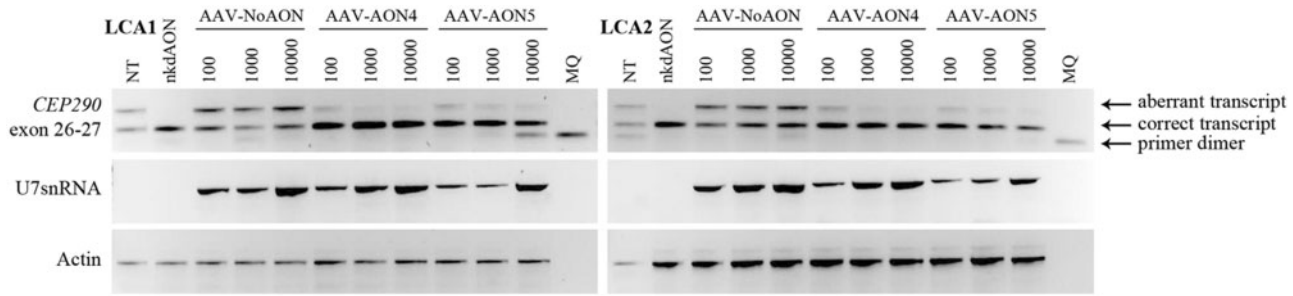

Figure 3. Splice correction efficacy of AON-containing AAVs. RT-PCR analysis on two different patient cell lines transduced with AAV-NoAON, AAV-AON4 or AAV-AON5, at three different MOIs (100, 1000 and 10 000). Amplification from exon 26 to exon 27 of *CEP290* revealed the presence of the aberrant transcript in the non-treated (NT) as well as the AAV-NoAON-transduced cells, while it was strongly decreased or completely absent in the AAV-AON4 and AAV-AON5-treated cells. Transfection of the naked AON (nkd AON) served as a positive control. U7snRNA amplification was used as a measure for the transduction efficacy, and actin as a loading control. MQ was the negative control of the PCR reaction while NT refers to non-transduced cells.

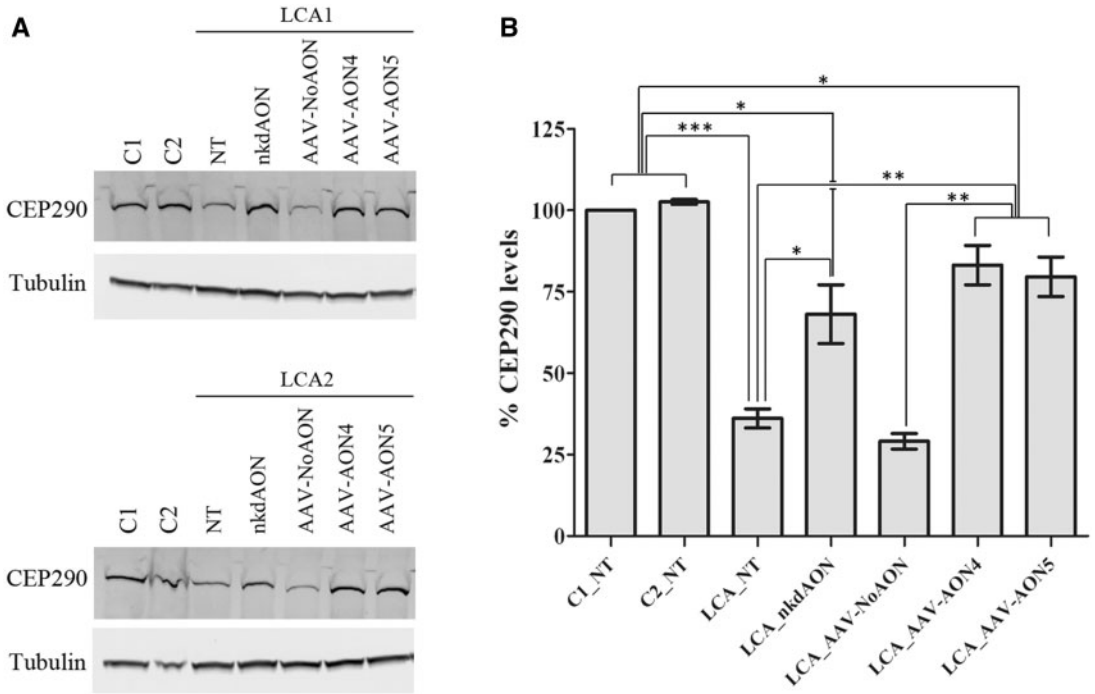

Figure 4. Assessment of CEP290 protein levels upon transduction of AON-containing AAVs (**A**) Immunodetection of CEP290 protein levels in treated and non-treated (NT) LCA fibroblast cells in comparison to the control fibroblast cells (C1 and C2). Tubulin detection was used for normalization. (**B**) Quantification of CEP290 protein levels shown in panel A. Values were normalized against tubulin. C1 was set up as a 100% and all samples were referred to this value. Naked AON (nkdAON) and AAV-AON4 and AAV-AON5 significantly increased the CEP290 protein levels. T-test was performed: *P-value < 0.05; **P-value < 0.01 and ***P-value < 0.001. Bars indicate SD.

or transduced with AAV-AON4 and AAV-AON5, showed a significant increase in CEP290 protein levels, almost reaching those observed in healthy controls (Fig. 4). Again, no differences were observed between the untransduced cells and those transduced with AAV-NoAON (Fig. 4). In addition, we studied the effect of AON transfection and AAV transduction in control fibroblasts, and no change in CEP290 protein levels was observed for any of the conditions tested (Supplementary Material, Fig. S2B).

CEP290 localizes in the basal body of the cilium and is thought to play an important role in cilium development and/or ciliary transport (7,30). When cultured under serum starving conditions, fibroblast cells develop cilia (31). When comparing the appearance of cilia in control fibroblasts versus fibroblasts of LCA patients with the intronic *CEP290* mutation, a clear ciliary phenotype was observed, i.e. a reduced number of ciliated cells, and a shorter average length of the cilium (Fig. 5). Remarkably, the fibroblast cells of the LCA patients displayed a high heterogeneity, showing three different appearances: no cilium, a short cilium or a normal cilium (Fig. 5A). Only the cells with a normal cilium showed a positive signal for CEP290 staining in the basal body, suggesting that the cilium length is directly correlated to a proper expression and localization of the CEP290 protein. In addition, this variability suggests that the 1:1 ratio of the aberrant and normal transcripts is an average of a population of cells, and may differ amongst individual cells. To assess whether the ciliary phenotype could be restored by AONs, fibroblast cells were again transfected (0.1 μmol/l) or transduced (MOI of 10 000) with AONs or AAV-AONs and subjected to serum starvation 48 h following transfection/transduction. Our results showed that the ciliary phenotype was

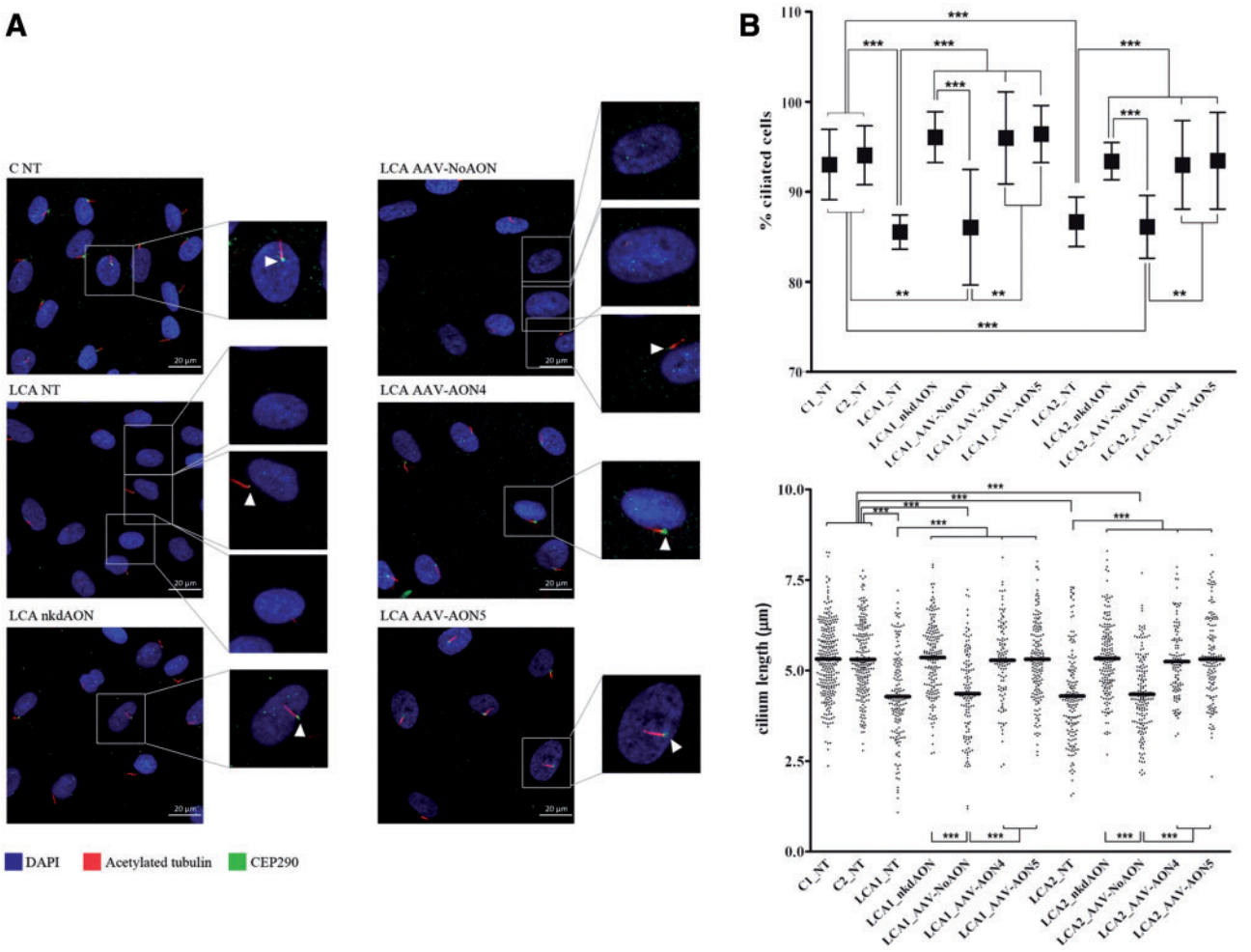

Figure 5. Immunocytochemical analysis of cilium integrity. (**A**) Immunocytochemistry in control (C) and patient (LCA) fibroblast cell lines. CEP290 (in green) localizes to the basal body of the cilia (as indicated by the head arrows). The cilium axoneme is stained with acetylated tubulin (in red) whereas the nuclei are stained with DAPI (blue). (**B**) Quantification of the percentage of ciliated cells and the length of the cilium in treated and untreated LCA cells compared to control (C1 and C2) cells. A minimum of 150 ciliated cells were measured for each condition and a Mann–Whitney test was used for statistic analysis. **P-value $\leq$ 0.01 and ***P-value $\leq$ 0.001. Bars indicate SD. No statistical difference was observed between control and patient samples that were treated with nkdAON or AAV-AONs.

completely rescued after 96 h treatment (Fig. 5A), i.e. the number of ciliated cells as well as the average length of the cilium returned to the values observed in control fibroblasts (Fig. 5B). Notably, the rescue of the ciliary phenotype was accompanied by a marked increase of CEP290 staining at the base of the cilium, as is apparent from the immunocytochemistry images presented in Figure 5A. No differences in ciliation and cilium length were observed following AON treatment in control cell lines (Supplementary Material, Fig. S2C).

Finally, we aimed to determine the *in vivo* efficacy of AAV-AONs and that of naked AON molecules when delivered to the retina. For that purpose, we used our humanized *Cep290* mouse model (*Cep290*$^{lca/lca}$) that contains exon 26, intron 26 with the c.2991 + 1655A > G mutation and exon 27 of the human *CEP290* gene. Previously, we showed that the cryptic splice site is recognized at low but detectable levels, although unfortunately no retinal phenotype was observed in these mice (32). Fibroblast cells derived from this mouse model were transduced with AAV2/2-AON4 and -AON5, to determine which AAV-AON was more effective in a mouse molecular environment. AON5 showed the highest efficacy (data not shown) and thus was packaged into an AAV2/9 which presents a high tropism for photoreceptor cells (33,34). Subsequently, naked AON, AAV2/9-NoAON and AAV2/9-AON5 were delivered to the transgenic mice by intraocular injections. In the first group, retinas were harvested after 10 days and analyzed at RNA level. RT-PCR analysis from left eyes (injected with phosphate buffered saline (PBS)) and right eyes (injected with the naked or AAV-packaged AON) revealed a statistically significant decrease of exon X in the mice treated with naked AONs as well as in the AAV-AON5 injected animals, and no differences in the animals that were administered AAV-NoAON (Fig. 6A and C). A total of ~50% and ~20% reduction of exon X-containing transcripts was observed for naked AON and AAV-AON5, respectively (Fig. 6E). The amplification of the U7snRNA supported the targeting of retinal cells (Fig. 6A and G). Of note, since we injected the AON within the modified mouse U7snRNA, endogenous levels of U7snRNA were detected in all samples. However, an additional shorter band (AAV-NoAON) and larger band (AAV-AON5) indicated the presence of our therapeutic molecule (Fig. 6A). Similar results were obtained when analyzing a group of animals 30 days after injection (Fig. 6B, D, F and H), indicating that the positive effect of a single delivery persists for a longer period of at least thirty days. To discard side effects of the delivery of these molecules to the retina, we performed toluidine blue staining in retinal sections from two animals 10

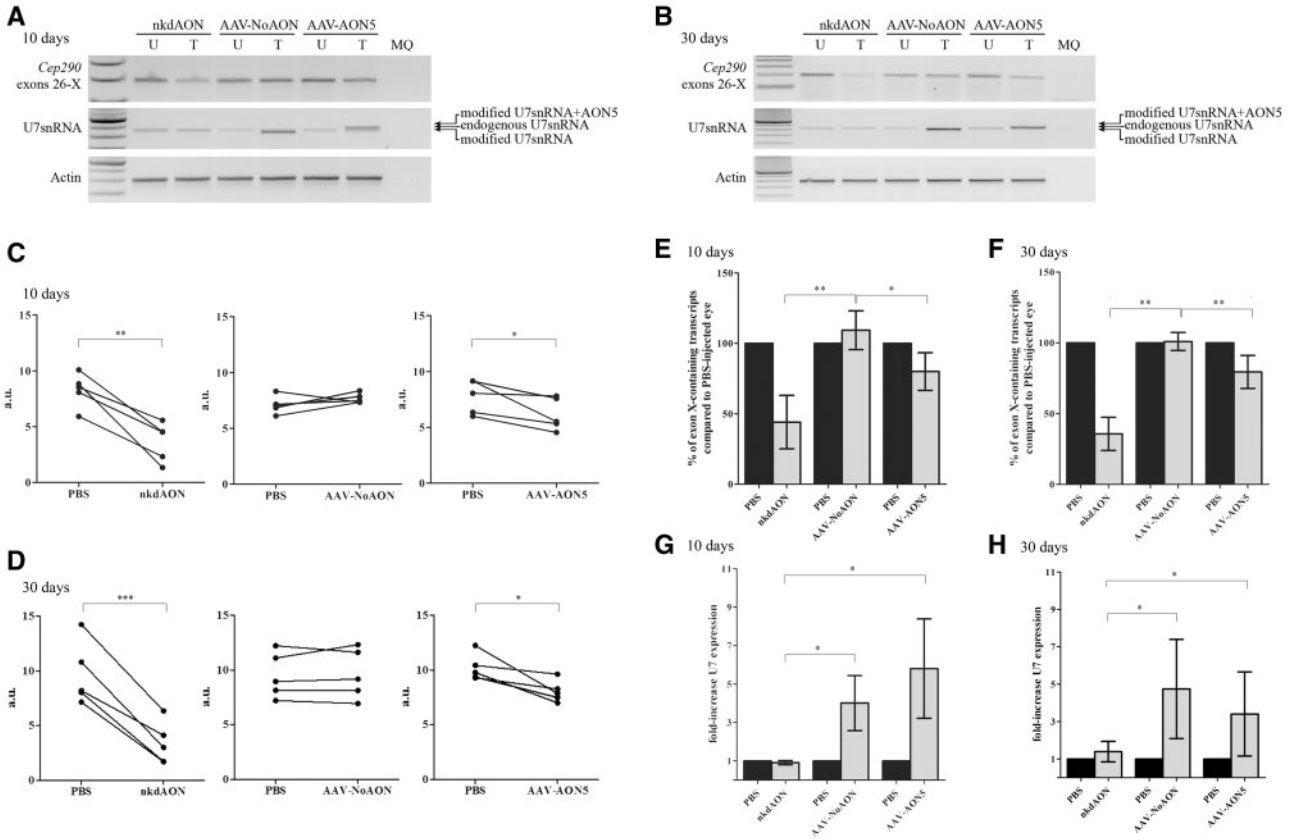

Figure 6. *In vivo* correction of aberrantly spliced *CEP290*. (**A** and **B**) Representative gel electrophoresis of the PCR reactions amplifying exon 26 to cryptic exon X, U7snRNA and actin (to normalize) of one of each replicate at (A) 10 days and (B) 30 days. MQ is the negative control of the PCR. 'U' stands for untreated and refers to PBS-injected retinas, whereas 'T' means treated and shows the effect on the AON or AAV-AON-injected retinas. (**C** and **D**) Schematic representation of the decrease of aberrant exon X in each replicate (C) at 10 days and (D) at 30 days. Bands were semi-quantified with ImageJ and normalized against actin. The Y axis indicated the arbitrary units (a.u.). (**E** and **F**) Percentage of aberrant exon X-containing transcripts at (E) 10 days and (F) 30 days. PBS-injected eyes were considered as a reference and placed at 100%. (**G** and **H**) Fold-increase of U7snRNA detection. PBS-injected retinas were taken as a reference and set at 1.0 at (G) 10 days and (H) 30 days. In all graphs, *P-value $\leq$ 0.05, **P-value $\leq$ 0.01 and ***P-value $\leq$ 0.001. Bars indicate SD. For statistical analysis of data represented in (C) and (D), a paired T-test was used, whereas for data shown in panels (E–H), a Mann–Whitney test was used.

days following AON administration. No morphological defects, such as photoreceptor degeneration, were detected (Supplementary Material, Fig. S3). In addition, to confirm that retinal structure was not compromised, we performed glial fibrillary acidic protein (GFAP) immunostaining. GFAP expression is an indicator of gliosis and is considered as stress marker in the retina (35). No differences were observed between PBS- or therapeutic-injected eyes (Supplementary Material, Fig. S4).

Discussion

Mutations in *CEP290* are the most common genetic cause of LCA in the Caucasian population, accounting for up to 20% of all cases (3). Intriguingly, an intronic founder mutation in *CEP290* (c.2991 + 1655A > G) explains 15% of all LCA cases in several Western countries, including the US, France, Belgium and The Netherlands (2,5,8,9), and shows a somewhat lower prevalence in other European countries (10). Therefore, *CEP290*, and in particular the intronic mutation, has emerged as an attractive target for developing genetic therapies. In this study, we show that delivery of AONs effectively rescues aberrant *CEP290* splicing *in vitro* and *in vivo*, highlighting the enormous potential of this therapeutic approach.

For several genetic subtypes of IRD, preclinical therapeutic intervention studies are ongoing, with encouraging results in many of these (36,37). In addition, clinical trials employing gene augmentation therapy have been initiated for several different genetic subtypes of IRD, e.g. caused by mutations in *ABCA4*, *CHM*, *MERTK*, *MYO7A* and *RPE65*. Subretinal delivery of AAVs carrying wild-type *RPE65* cDNA to the retinal pigment epithelium showed, besides moderate improvement in visual function (11–14), a high safety profile, with limited risk of insertional mutagenesis, and very low or benign immune responses to the AAV, even upon readministration of the vector to the second eye (38). More recently, AAV delivery of *CHM* cDNA also was shown to be safe and moderately effective in six treated patients with choroideremia (16). A serious constraint of AAVs however is their limited cargo capacity, as only transgenes smaller than 5 kb can be efficiently packaged in these vectors (36). Therefore, many large genes are not eligible for AAV-mediated delivery, as is the case for *CEP290* whose coding sequence is ~7.5 kb long. Recently, dual AAV strategies have been developed that consist of delivering two different AAV vectors, each containing half of the cDNA with a small overlapping region, allowing the assembly of the complete transcript in the target cell following transduction. Although promising results have been obtained in reconstituting full-length cDNAs of *ABCA4* and

MYO7A in mutant mouse models for Stargardt disease and Usher syndrome type 1B, respectively (39,40), not much success has been achieved so far for *CEP290* (Renee C. Ryals, personal communication at ARVO Annual Meeting 2014). Alternatively, lentiviral vectors that can carry cargos up to 10 kb (36), sufficient for packaging the full-length *CEP290* cDNA, could be used. A disadvantage of lentiviruses however is that they integrate into the genome of the host cell, running the risk of insertional mutagenesis. In addition, they do not efficiently target differentiated photoreceptor cells which is the primary target for a *CEP290* gene therapy. Another problem associated with gene augmentation is the fact that expression levels cannot be regulated, therefore increasing the risk of toxicity upon reaching expression levels exceeding those of the endogenous protein. Recently, it was shown that transduction of lentiviruses containing wild-type *CEP290* cDNA under control of a CMV promoter could rescue a ciliary phenotype in patient-derived fibroblast cells, although in the same study, toxic effects were observed upon transduction of these lentiviruses in other cell types (41). Together, these studies suggest that there are many challenges associated with developing gene augmentation therapy for *CEP290*-associated LCA. AON therapy does not have these limitations, as the small AON sequences easily fit into AAVs, and since the endogenous mRNA is the therapeutic target, the maximum expression levels of the wild-type protein will never exceed that of the endogenous protein.

In this study, we employed patient-derived fibroblast cells and a humanized mutant *Cep290* mouse as model systems to assess the efficacy of AAV-based and naked AON delivery. Fibroblasts endogenously express the CEP290 protein and develop cilia under serum starvation conditions, and thus are a good model for *in vitro* studies. Although these cells are hard to transfect with plasmid DNA, transduction of AAVs was very efficient. When testing a panel of different AAV serotypes, AAV2/2 appeared to show the highest tropism for fibroblasts, although AAV2/5 and AAV2/9 also showed affinity for these cells. With respect to future clinical applications, we also considered the fact that both AAV2/5 and AAV2/9 have a higher tropism for photoreceptor cells than AAV2/2 (33,42), and that AAV2/9 is particularly efficient at transducing cone photoreceptors, which degenerate later in the course of the disease in humans (43). Nevertheless, in order to have the optimal vector for the studies in our fibroblast model, AAV2/2 was selected for the generation of the AON-containing vectors. In our experimental design, effective AON sequences were subcloned into a modified U7snRNA gene, a strategy that has previously been shown to be effective in redirecting splicing of the *DMD* gene (29). Presumably, the same construct is also effective in redirecting splicing in the context of a photoreceptor cell, ultimately the target cell for therapeutic intervention.

Despite the suitability of the fibroblast cells as a preclinical model to assess the therapeutic efficacy of AON-based therapy, ideally one would like to study its potential in the context of a living animal. Previously, we generated a humanized transgenic knock-in mouse model where part of the mouse *Cep290* genomic DNA was replaced by its orthologous human counterpart, i.e. exon 26, intron 26 (including the LCA-causing mutation) and exon 27, in order to assess the therapeutic efficacy of AON therapy *in vivo*. However, despite a correct genetic engineering of the transgenic mouse model, only a low amount of aberrant splicing of *Cep290* mRNA was observed, insufficient to compromise retinal function (32). Yet, the presence of exon X-containing transcripts did allow to study whether AON administration to the retina of these mice could redirect *CEP290* splicing. Delivery of AONs, both as naked molecules or packaged into AAVs, resulted in a statistically significant decrease in the amount of exon X-containing transcripts, either at 10 days or 30 days after delivery, although the effect was stronger for the naked AON molecules. There are a few explanations for this. First, the delivery of naked AONs can be performed via intravitreal injections, since AONs are small molecules that can penetrate all retinal cell layers and thus easily reach the photoreceptor cells. In contrast, the delivery of AAVs requires subretinal injections, with which only a part of the retina can be targeted (20–60% depending on the injection), and thereby increases the variability of each experiment. Indeed, we observed more variability in the decrease of exon X in mice treated with AAV-AONs compared to those with the naked AON molecule where all replicates showed similar results. In addition, U7snRNA expression levels also supported the variability observed in the delivery of AAVs into murine retina, as shown in the error bars of Figure 6G and H, where one of the replicates showed a ~6-fold increased expression of U7snRNA. Another possibility is that the modified U7snRNA might show a different efficacy between humans and mice, as we observed a less efficient rescue in *Cep290*$^{lca/lca}$ fibroblasts when transduced with AAV-AONs compared to the human fibroblasts under similar conditions. Taken together, although of course ideally our mouse model would have had a retinal phenotype that could be delayed/rescued following AON delivery, the intraocular administration of AONs shows that these molecules are able to redirect splicing in the ultimate target tissue for therapeutic intervention, and thus hold great promise for the treatment of LCA caused by this particular mutation.

So far, AONs have been used in clinical trials for other ocular diseases such as CMV-induced retinitis to decrease the viral load in AIDS patients (Vitravene®), or diabetic macula edema and diabetic retinopathy to downregulate *c-Raf* expression and thereby decrease neovascularization (iCo-007) (23). In addition, a systemic delivery of AONs was recently shown to be successful in a humanized mouse model for Usher syndrome type 1C, characterized by a combination of hearing deficits, vestibular impairment and retinal dystrophy. Intraperitoneal injection of naked AONs targeting a cryptic splice site caused by a recurrent mutation in *Ush1C*, resulted in an increased level of correctly spliced *Ush1C* mRNA, and a strong improvement in auditory and vestibular function in these mice (44). A systemic delivery of AONs, whether as naked molecules or packaged in AAVs, however, would require high amounts of AON and increase the chances of evoking immune responses. The fact that the eye is an immune-privileged organ that is tightly regulated to preserve its integrity (45), confers the possibility to deliver the AON molecules directly to the retina, either by intravitreal or subretinal injections with minimal toxic immunological side effects (36). Very recently, two publications showed the safety and efficacy of delivering AONs to the retina. In one of the studies delivery of naked molecules targeting regular exons of *Cep290* to the mouse retina resulted in some skipping of the targeted exon. In addition, these AON molecules reached all retinal layers and no adverse effects were detected (46). In the other study, AONs were employed to degrade the mutant *RHO* allele in autosomal dominant retinitis pigmentosa in rats (47). However, the chemistry of the AONs in the last study differed from the frequently used phosphorothioate backbone AONs (2′-O-methyl) by introducing a 2′-O-methoxyethyl modification at different positions. Modifications in AONs are frequently used to modify the properties and function (splice modulation, RNA degradation, etc.) of these molecules, as well as their stability, penetration capacity and susceptibility to RNases amongst others (48).

In terms of future therapeutic intervention in humans, there are several pros and cons to either an AAV-based administration of AONs, or delivery of AONs as a naked molecule. Due to their small size, naked AONs may be able to penetrate and reach the photoreceptor cells in the retina more readily upon intravitreal injections, compared to the subretinal delivery of currently used AAVs. Also, as naked AONs have a limited stability (ranging from weeks to months depending on the modifications added to the oligonucleotide), potential negative side effects of the AONs would likely also be transient. Nevertheless, the use of naked AONs would require repeated, life-long injections, as *CEP290*-associated LCA manifests in childhood. In contrast, a single administration of an effective AAV could give therapeutic benefit for many years, potentially life-long. And although with current approaches, only part of the retina is targeted, new subclasses of AAVs are currently being developed that might allow a more effective targeting of the outer retina after intravitreal injection (49,50).

One other aspect that determines future therapeutic success is the status of degeneration of the retina at the time of treatment. Despite the early-onset and severe nature of the visual impairment in *CEP290*-associated LCA, the integrity of the photoreceptor layer appears to be relatively well conserved in some patients with *CEP290*-associated LCA, up to young adulthood (51,52). The same is true for the connections of the visual pathway in the brain, giving hope that these patients are able to process and interpret the visual input that would become available following effective treatment (51). Despite this therapeutic window of opportunity, previous studies have shown a clear correlation between the age of treatment and therapeutic outcome (13), suggesting that LCA patients with *CEP290*-associated LCA may benefit most from early treatment.

In conclusion, we here show the therapeutic efficacy of AAV-mediated delivery of AONs to treat the most common genetic form of childhood blindness, i.e. *CEP290*-associated LCA. In fibroblast cells from LCA patients, aberrant *CEP290* splicing was corrected, CEP290 protein levels were restored, and a ciliary phenotype was completely rescued following AON administration. In mouse retinas of a humanized *Cep290* mouse model carrying the LCA mutation, naked as well as AAV-mediated delivery of AONs decreased the amount of aberrant *Cep290* transcripts, demonstrating that both AON delivery methods provide an excellent treatment strategy for *CEP290*-associated LCA. With that, AON-based therapy could be an effective way to halt the progression or even improve visual function in many visually impaired individuals worldwide.

Materials and Methods

Study design

The objective of this work is to assess the efficacy of AON-based splice correction therapy for *CEP290*-associated LCA, and compare delivery of AONs either as naked molecules or packaged into AAVs. Fibroblast cell lines derived from two unrelated LCA patients homozygously carrying the c.2991+1655A>G mutation, and from two age- and gender-matched healthy individuals were used. Outcome measures include the correction of aberrant *CEP290* splicing via RT-PCR, the assessment of CEP290 protein levels via Western blot analysis, and a qualitative and quantitative characterization of cilium structure via immunofluorescence microscopy. All experiments were performed simultaneously in all cell lines. In addition, intraocular injections of naked AON molecules or AAVs were performed in a humanized mouse model carrying the intronic *CEP290* mutation (32). Right eyes were injected with the therapeutic molecule, while contralateral left eyes were injected with PBS and used as a control. Two different time points were selected for the study, 10 and 30 days. The relative abundance of exon X-containing *Cep290* transcripts was determined by PCR and retinal morphology and gliosis were assessed to detect whether the retinal structure was compromised. In total, 10–12 animals were injected per experimental group for each time point. All graphs represent the average ± SD.

Ethics statement

Our research was conducted according to the tenets of the Declaration of Helsinki. The procedures for obtaining human skin biopsies to establish primary fibroblasts cell lines were approved by the Ethical Committee of the Radboud University Medical Centre (*Commissie Mensgebonden Onderzoek* Arnhem-Nijmegen). Written informed consent was gathered from all participating individuals by signing the Declaration of Permission for the Use of Body Material (*Toestemmingsverklaring gebruik lichaamsmateriaal*) of the Radboud University Medical Centre. All animal experiments were performed after obtaining approval from the Radboud University Nijmegen ethics committee for experimental animal research (RU-DEC-2014-073), and according to the regulations of the ARVO statement for the use of animals in ophthalmic and vision research. All procedures were carried out in the Netherlands.

Construct design

AON sequences were cloned into a modified U7snRNA gene in the pSMD2 shuttle vector that contains the ITR sequences for AAV production, via a two-step PCR approach as described elsewhere (29). This yielded six different AON-containing vectors, coined pAAV-AON1 to pAAV-AON6 and one control vector (Fig. 1A). Previously, we cloned a ~6.4 kb fragment of the *CEP290* gene that contained part of intron 25, exon 26, intron 26 (either with or without the intronic mutation), exon 27 and part of intron 27 (32), and inserted into the pCI-Neo plasmid flanked by the exon 3 and 5 of the *RHO* gene (53).

Cell culture and transfection

Fibroblast cell lines derived from skin biopsies of individuals with *CEP290*-associated LCA or healthy controls were cultured in DMEM, supplemented with 20% fetal bovine serum (FBS), 1% penicillin–streptomycin and 1% of sodium pyruvate at 37 °C and 5% CO_2. HEK293T cells were cultured in DMEM supplemented with 10% FBS, 1% penicillin–streptomycin and 1% sodium pyruvate at 37°C and 5% CO_2.

In order to validate the efficacy of the AON-containing vectors, serial dilutions were carried out by co-transfecting 1 μg of the LCA minigene construct, together with various amounts of each pAAV-AON vector (0.5 μg, 0.125 μg and 0.035 μg) in human embryonic kidney (HEK293T) cells. Co-transfections were performed by combining the two plasmids with FuGene (Promega, Madison, WI) reagent (1:3 ratio) following manufacturer's protocol. Naked AON (0.1 μmol/l) was used as a positive control. Cells were harvested for transcriptional analysis 48 h post-transfection.

AON-containing AAV generation

For the studies in fibroblasts, the two most effective AON constructs were selected for AAV2/2 production, whereas the AON construct most effective in mouse cell lines, was selected for AAV2/9 generation. Plasmid DNA was purified by the Megaprep kit (Qiagen, Venlo, The Netherlands). The U7snRNA-AON constructs were packaged into AAV by transfection of three plasmids (AAV pSMD2 plasmid containing the U7snRNA-AON, AAV package plasmid encoding AAV Rep and Cap proteins from serotypes 2 or 9 and adenovirus helper plasmid) in HEK293 cells. Three days after transfection, cells and culture medium were collected and enzymatically treated with Benzonase at high salt concentration (0.5M NaCl). The cell debris was removed by high speed centrifugation and regular filtration. The supernatant went through a tangential flow filter which concentrated the viral solution. Recombinant AAV vector particles were isolated and extracted by running the concentrated supernatant through the iodixanol density gradient. The purified supernatant was then further concentrated by running through an Amicon filter with a 100 000 molecular weight cut off. The AAV titer was determined by real-time PCR and the purity was verified by SDS–PAGE. For assessing which AAV serotype most effectively transduces fibroblast cells, an existing panel of AAVs containing an expression cassette of GFP under control of the CMV promoter was used.

AAV transduction in fibroblasts

Fibroblast cell lines were transfected or transduced as follows. For transfection, cells were seeded in the corresponding plate according to the amount of cells needed and transfected with 0.1 μmol of naked AON using FuGene HD (Promega, Madison, WI) as described before. For transduction, cells were transduced with AAV at different MOIs. (100, 1000 and 10 000) and medium was replaced after 24 h. Cells were harvested 96 h later for transcriptional analysis. For protein and immunocytochemistry studies cells were transduced with a MOI of 10 000 or transfected with 0.1 μmol of naked AON. For protein analysis 1 800 000 cells were seeded in 10 cm dishes and harvested 96 h following transfection/transduction. For immunocytochemistry, fibroblast cells were seeded on coverslips in a 12-well plate and 48 h following transfection/transduction, medium was replaced for a low FBS (0.2%) containing medium for another 48 h.

Intraocular injections

Intravitreal (for naked AONs) and subretinal (for AAVs) injections were performed on a humanized *Cep290* mouse model carrying the intronic *Cep290* mutation (32). For each therapeutic molecule (naked molecule (nkdAON), AAV2/9-U7snRNA-NoAON (AAV-NoAON) or AAV2/9-U7snRNA-AON (AAV-AON5) and time point (10 or 30 days), ten to twelve animals were used. Mice were anesthetized using isofluorene (also continuously administered during the surgical procedure) and analgesia (Carprofen, 5-10 mg/kg) was injected subcutaneously. Three microliters of naked AON (20 μg/μl), AAV-NoAON and AAV-AON ($\sim 3 \times 10^{12}$ genome copies/ml for each) were injected in the right eye, whereas 3 μl of PBS were injected in each left eye. Retinas were harvested either 10 days or 30 days post-injection. Ten animals were used for RNA analysis, while in addition, for the 10-days group, two mice were employed to assess retinal morphology. In order to obtain sufficient amounts of RNA, two retinas were pooled per group, yielding five biological replicates for each molecule.

RNA isolation and RT-PCR analysis

RNA was isolated from fibroblast cells using the Nucleospin RNA II isolation kit (Machery Nagel, Düren, Germany) following the manufacturer's protocol. Five hundred nanograms of RNA were used for cDNA synthesis by using the iScript cDNA Synthesis kit (Bio-Rad, Hercules, CA) at a final volume of 20 μl and then diluted 3.5 times by adding 50 μl of RNAse-free H_2O. All the PCR reaction mixtures (25 μl) contained 10 μM of each primer pair, 2 μM of dNTPs, 1.5 mM $MgCl_2$, 10% Q-solution (Qiagen, Venlo, Netherlands), 1 U of *Taq* polymerase (Roche, Penzberg, Germany) and 5 μl of diluted cDNA. PCR conditions were 94 °C for 2 min, followed by 35 cycles of 20 s at 94 °C, 20 s at 58 °C and 35 s at 72 °C, with a final extension step of 2 min at 72 °C. Amplicons were analyzed by agarose gel electrophoresis. Actin expression was used to compare and normalize samples. For co-transfection of the minigene with the AON vectors, RHO and U7 primers were used to assess the transfection efficiency. All oligonucleotide sequences are listed in Supplementary Material, Table S1. For *in vivo* experiments, retinas were first disrupted and RNA was isolated as described above. For cDNA synthesis, 1 μg of RNA was used. PCR reactions were performed as described above.

Western blot analysis

Fibroblast cells were homogenized in 100 μl of RIPA buffer (50 mM Tris pH 7.5, 1 mM EDTA, 150 mM NaCl, 0.5% Na-Deoxycholate, 1% NP40 plus protease inhibitors). Total protein was quantified using the BCA kit (Thermo Fisher Scientific, Waltham, MA). For CEP290 detection, ~75 μg of total protein lysate supplemented with sample buffer was loaded onto a NuPage 3–8% tris-acetate gel (Life technologies, Carlsbad, CA). The electrophoresis was carried out for 4 h at 150 V. For normalization, ~25 μg of the same protein lysates were loaded onto a NuPage 4–12% bis-acrylamide tris-glycine gel (Life technologies, Carlsbad, CA) for detection of α-tubulin and run for 2 h at 150 V. All lysates were boiled for 5 min at 98 °C prior to loading. Proteins were transferred to a PVDF membrane (GE Healthcare, Little Chalfont, UK) overnight at 25 V and 4 °C in transfer buffer containing 10% methanol and 0,1% SDS. Blots were blocked in 5% non-fat milk in PBS for 6 h at 4 °C, incubated overweekend at 4 °C with rabbit anti-CEP290 (dilution 1:1000, Novus Biological, Littleton, CO) or mouse anti-α-tubulin (dilution 1:2000, Abcam, Cambridge, UK) in 0.5% non-fat milk in PBS solution, washed in PBS with 0.1% Tween-20 (PBST) (4 × 5 min), incubated with the appropriate secondary antibody for 1 h at room temperature (RT), washed in PBST (4 × 5 min) and developed using the Odyssey Imaging System (Li-Cor Biosciences, Lincoln, NE). Semi-quantification was performed using Image J software (54).

Immunofluorescence analysis on cells

Cells were grown on coverslips in 12 well plates and transfected with 0.1 μmol of naked AON or transduced with AAVs (MOI of 10 000). After 48 h of serum starvation, cells were rinsed with 1× PBS (137 mM NaCl, 2.7 mM KCl, 1.5 mM KH_2PO_4, and 8 mM Na_2HPO_4, pH 7.4), fixed in 2% paraformaldehyde for 20 min, permeabilized in PBS with 1% Triton X for 5 min and blocked for 30 min with 2% bovine serum albumin in PBS at RT. Primary antibody was diluted in blocking solution and incubated for 90 min

at RT. Subsequently, slides were washed 5 min in PBS three times, incubated with 1:500 dilution of the corresponding Alexa Fluor-conjugated antibody (Molecular Probes, Eugene, OR) for 45 min. Finally, slides were washed in PBS 3 × 5 min and mounted in Vectashield with DAPI (Vector laboratories, Burlingame, CA). Primary antibodies dilutions were 1:1000 for mouse anti-acetylated tubulin (Sigma-Aldrich, St. Louis, MO) and 1:300 for rabbit anti-CEP290 (Novus Biological, Littleton, CO). Pictures were taken at 40× with Axio Imager (Zeiss, Oberkochen, Germany) microscope. For each condition, at least 150 ciliated cells were counted and their cilia were measured using Image J software (54).

Morphological and immunohistochemical analysis

Eyes from injected mice were enucleated and fixed in 4% PFA for 10 min at RT. Cornea and lens were removed and eyecups were fixed in 2% PFA 2 h at RT. Subsequently, samples were washed three times in PBS, incubated in a 20% sucrose solution for 1 h at 4 °C, 1 h in a 30% sucrose solution at 4 °C and 16 h in 40% sucrose at 4 °C. Eyecups were oriented and embedded in OCT (Tissue-Tek, Sakura Finetech, Torrance, CA). Seven micron cryosections were used for morphological and immunohistochemical analyses. Morphology was assessed by staining the sections with toluidine blue. For immunostaining, gliosis marker GFAP (rabbit polyclonal anti-GFAP, Dako, Heverlee, Belgium) was used. Briefly, sections were dried for 1 h at RT, permeabilized for 20 min in 0.01% Tween in PBS and blocked for 30 min (0.1% ovalbumin and 0.5% fish gelatine in PBS). Primary antibody incubation (dilution 1:1000 in blocking solution) was performed overnight at 4 °C. Sections were washed in PBS (4 × 5 min), and incubated for 1 h at RT with DAPI and Alexa Fluor 488-conjugated anti-rabbit secondary antibody (Life Technologies, Carlsbad, CA), washed in PBS (4 × 5 min), rinsed in water and mounted in Prolong Gold antifade kit (Life Technologies, Carlsbad, CA). Pictures were taken at 5x (Supplementary Material, Fig. S3A) or 20× (Supplementary Material, Fig. S3B and S4) with Axio Imager (Zeiss, Oberkochen, Germany) microscope.

Statistical analysis

In order to study the differences between treated and untreated cells we applied the two-tailed Student's T and Mann–Whitney tests. *P*-values smaller than 0.05 were considered significant as indicated in the figures. Statistical analysis was performed for the quantification of the CEP290 protein levels, as well as the ciliation and cilium length measurements. For the assessment of the efficacy *in vivo* a paired Student's T test was performed to determine statistical significance of the decrease in each replicate, while a Mann–Whitney test was used to compare groups.

Supplementary Material

Supplementary Material is available at *HMG* online.

Acknowledgements

We gratefully acknowledge the LCA patients that donated skin biopsies for this study. We would like to thank Drs. L. Ingeborgh van den Born, B. Jeroen Klevering and Charlotte Ockeloen for clinical activities, Stefanie Schönfeld, Mike Peters, Lisette Hetterschijt, Sylvia E. Van Beersum and Saskia D. van der Velde-Visser for technical assistance, and Dr. Aurelie Goyenvalle for providing the pSMD2 construct.

Conflicts of interest statement. R.W.J.C. is an inventor on a filed patent (P6037013PCT) that is related to the contents of this manuscript. J.B. is a founder of Gensight Biologics, serves on a DSMC for Genzyme/Sanofi and is a scientific member of a team that has a clinical trial agreement with Spark Therapeutics. L.H.V. is an inventor on patents related to AAV gene therapy, has served as a consultant and is inventor on technologies licensed to biotechnology and pharmaceutical industry, and is co-founder and consultant to GenSight Biologics. All other co-authors have no conflict of interest.

Funding

This work is financially supported by the Netherlands Organisation for Scientific Research (NWO) (VENI 916.10.096), the Foundation Fighting Blindness (FFB) USA (TA-GT-0912-0582-RAD), FP7-PEOPLE-2012-ITN programme EyeTN, Brussels, Belgium (agreement no.: 317472), the JANIVO stichting, the Stichting August F. Deutman Researchfonds Oogheelkunde, the Rotterdamse Vereniging Blindenbelangen, the Algemene Nederlandse Vereniging ter Voorkoming van Blindheid, the Gelderse Blindenstichting, the Stichting Winckel-Sweep and the Stichting Nederlands Oogheelkundig Onderzoek (all to R.W.J.C.), FFB (C-GT-09130627-UPA02) to J.B., the NIH (DP1-OD008267) to J.B. and L.H.V., the Curing Kids Fund, FFB (TA-GT-0611-0571) and the Grousbeck Family Foundation (all to L.H.V.).

References

1. Koenekoop, R.K. (2004) An overview of Leber congenital amaurosis: a model to understand human retinal development. *Surv. Ophthalmol.*, **49**, 379–398.
2. Stone, E.M. (2007) Leber congenital amaurosis—a model for efficient genetic testing of heterogeneous disorders: LXIV Edward Jackson Memorial Lecture. *Am. J. Ophthalmol.*, **144**, 791–811.
3. den Hollander, A.I., Roepman, R., Koenekoop, R.K. and Cremers, F.P. (2008) Leber congenital amaurosis: genes, proteins and disease mechanisms. *Prog. Retin. Eye Res.*, **27**, 391–419.
4. Coppieters, F., Lefever, S., Leroy, B.P. and De Baere, E. (2010) *CEP290*, a gene with many faces: mutation overview and presentation of *CEP290* base. *Hum. Mutat.*, **31**, 1097–1108.
5. den Hollander, A.I., Koenekoop, R.K., Yzer, S., Lopez, I., Arends, M.L., Voesenek, K.E., Zonneveld, M.N., Strom, T.M., Meitinger, T., Brunner, H.G. *et al.* (2006) Mutations in the *CEP290* (*NPHP6*) gene are a frequent cause of Leber congenital amaurosis. *Am. J. Hum. Genet.*, **79**, 556–561.
6. Nagase, T., Ishikawa, K., Nakajima, D., Ohira, M., Seki, N., Miyajima, N., Tanaka, A., Kotani, H., Nomura, N. and Ohara, O. (1997) Prediction of the coding sequences of unidentified human genes. VII. The complete sequences of 100 new cDNA clones from brain which can code for large proteins in vitro. *DNA Res.*, **4**, 141–150.
7. Craige, B., Tsao, C.C., Diener, D.R., Hou, Y., Lechtreck, K.F., Rosenbaum, J.L. and Witman, G.B. (2010) CEP290 tethers flagellar transition zone microtubules to the membrane and regulates flagellar protein content. *J. Cell Biol.*, **190**, 927–940.
8. Coppieters, F., Casteels, I., Meire, F., De Jaegere, S., Hooghe, S., van Regemorter, N., Van Esch, H., Matuleviciene, A., Nunes, L., Meersschaut, V. *et al.* (2010) Genetic screening of

LCA in Belgium: predominance of *CEP290* and identification of potential modifier alleles in *AHI1* of *CEP290*-related phenotypes. *Hum. Mutat.*, **31**, E1709–E1766.
9. Perrault, I., Delphin, N., Hanein, S., Gerber, S., Dufier, J.L., Roche, O., Defoort-Dhellemmes, S., Dollfus, H., Fazzi, E., Munnich, A. *et al.* (2007) Spectrum of *NPHP6/CEP290* mutations in Leber congenital amaurosis and delineation of the associated phenotype. *Hum. Mutat.*, **28**, 416.
10. Vallespin, E., Lopez-Martinez, M.A., Cantalapiedra, D., Riveiro-Alvarez, R., Aguirre-Lamban, J., Avila-Fernandez, A., Villaverde, C., Trujillo-Tiebas, M.J. and Ayuso, C. (2007) Frequency of *CEP290* c.2991_1655A>G mutation in 175 Spanish families affected with Leber congenital amaurosis and early-onset retinitis pigmentosa. *Mol. Vis.*, **13**, 2160–2162.
11. Hauswirth, W.W., Aleman, T.S., Kaushal, S., Cideciyan, A.V., Schwartz, S.B., Wang, L., Conlon, T.J., Boye, S.L., Flotte, T.R., Byrne, B.J. *et al.* (2008) Treatment of leber congenital amaurosis due to *RPE65* mutations by ocular subretinal injection of adeno-associated virus gene vector: short-term results of a phase I trial. *Hum. Gene Ther.*, **19**, 979–990.
12. Jacobson, S.G., Cideciyan, A.V., Ratnakaram, R., Heon, E., Schwartz, S.B., Roman, A.J., Peden, M.C., Aleman, T.S., Boye, S.L., Sumaroka, A. *et al.* (2012) Gene therapy for leber congenital amaurosis caused by *RPE65* mutations: safety and efficacy in 15 children and adults followed up to 3 years. *Arch. Ophthalmol.*, **130**, 9–24.
13. Maguire, A.M., High, K.A., Auricchio, A., Wright, J.F., Pierce, E.A., Testa, F., Mingozzi, F., Bennicelli, J.L., Ying, G.S., Rossi, S. *et al.* (2009) Age-dependent effects of *RPE65* gene therapy for Leber's congenital amaurosis: a phase 1 dose-escalation trial. *Lancet*, **374**, 1597–1605.
14. Maguire, A.M., Simonelli, F., Pierce, E.A., Pugh, E.N. Jr., Mingozzi, F., Bennicelli, J., Banfi, S., Marshall, K.A., Testa, F., Surace, E.M. *et al.* (2008) Safety and efficacy of gene transfer for Leber's congenital amaurosis. *N. Engl. J. Med.*, **358**, 2240–2248.
15. Bainbridge, J.W., Smith, A.J., Barker, S.S., Robbie, S., Henderson, R., Balaggan, K., Viswanathan, A., Holder, G.E., Stockman, A., Tyler, N. *et al.* (2008) Effect of gene therapy on visual function in Leber's congenital amaurosis. *N. Engl. J. Med.*, **358**, 2231–2239.
16. MacLaren, R.E., Groppe, M., Barnard, A.R., Cottriall, C.L., Tolmachova, T., Seymour, L., Clark, K.R., During, M.J., Cremers, F.P., Black, G.C. *et al.* (2014) Retinal gene therapy in patients with choroideremia: initial findings from a phase 1/2 clinical trial. *Lancet*, **383**, 1129–1137.
17. Hammond, S.M. and Wood, M.J. (2011) Genetic therapies for RNA mis-splicing diseases. *Trends Genet.*, **27**, 196–205.
18. Goemans, N.M., Tulinius, M., van den Akker, J.T., Burm, B.E., Ekhart, P.F., Heuvelmans, N., Holling, T., Janson, A.A., Platenburg, G.J., Sipkens, J.A. *et al.* (2011) Systemic administration of PRO051 in Duchenne's muscular dystrophy. *N. Engl. J. Med.*, **364**, 1513–1522.
19. van Deutekom, J.C., Janson, A.A., Ginjaar, I.B., Frankhuizen, W.S., Aartsma-Rus, A., Bremmer-Bout, M., den Dunnen, J.T., Koop, K., van der Kooi, A.J., Goemans, N.M. *et al.* (2007) Local dystrophin restoration with antisense oligonucleotide PRO051. *N. Engl. J. Med.*, **357**, 2677–2686.
20. Erba, H.P., Sayar, H., Juckett, M., Lahn, M., Andre, V., Callies, S., Schmidt, S., Kadam, S., Brandt, J.T., Van Bockstaele, D. *et al.* (2013) Safety and pharmacokinetics of the antisense oligonucleotide (ASO) LY2181308 as a single-agent or in combination with idarubicin and cytarabine in patients with refractory or relapsed acute myeloid leukemia (AML). *Invest. New Drugs*, **31**, 1023–1034.
21. Tolcher, A.W., Kuhn, J., Schwartz, G., Patnaik, A., Hammond, L.A., Thompson, I., Fingert, H., Bushnell, D., Malik, S., Kreisberg, J. *et al.* (2004) A Phase I pharmacokinetic and biological correlative study of oblimersen sodium (genasense, g3139), an antisense oligonucleotide to the bcl-2 mRNA, and of docetaxel in patients with hormone-refractory prostate cancer. *Clin. Cancer Res.*, **10**, 5048–5057.
22. Gebhard, C., Huard, G., Kritikou, E.A. and Tardif, J.C. (2013) Apolipoprotein B antisense inhibition–update on mipomersen. *Curr. Pharm. Des.*, **19**, 3132–3142.
23. Hnik, P., Boyer, D.S., Grillone, L.R., Clement, J.G., Henry, S.P. and Green, E.A. (2009) Antisense oligonucleotide therapy in diabetic retinopathy. *J. Diabetes Sci. Technol.*, **3**, 924–930.
24. Collin, R.W., den Hollander, A.I., van der Velde-Visser, S.D., Bennicelli, J., Bennett, J. and Cremers, F.P. (2012) Antisense Oligonucleotide (AON)-based Therapy for Leber Congenital Amaurosis caused by a frequent mutation in *CEP290*. *Mol. Ther. Nucleic Acids*, **1**, e14.
25. Gerard, X., Perrault, I., Hanein, S., Silva, E., Bigot, K., Defoort-Delhemmes, S., Rio, M., Munnich, A., Scherman, D., Kaplan, J. *et al.* (2012) AON-mediated Exon Skipping Restores Ciliation in Fibroblasts harboring the common Leber Congenital Amaurosis *CEP290* mutation. *Mol. Ther. Nucleic Acids*, **1**, e29.
26. Dias, N. and Stein, C.A. (2002) Antisense oligonucleotides: basic concepts and mechanisms. *Mol. Cancer Ther.*, **1**, 347–355.
27. Stieger, K., Schroeder, J., Provost, N., Mendes-Madeira, A., Belbellaa, B., Le Meur, G., Weber, M., Deschamps, J.Y., Lorenz, B., Moullier, P. *et al.* (2009) Detection of intact rAAV particles up to 6 years after successful gene transfer in the retina of dogs and primates. *Mol. Ther.*, **17**, 516–523.
28. Acland, G.M., Aguirre, G.D., Bennett, J., Aleman, T.S., Cideciyan, A.V., Bennicelli, J., Dejneka, N.S., Pearce-Kelling, S.E., Maguire, A.M., Palczewski, K. *et al.* (2005) Long-term restoration of rod and cone vision by single dose rAAV-mediated gene transfer to the retina in a canine model of childhood blindness. *Mol. Ther.*, **12**, 1072–1082.
29. Goyenvalle, A., Vulin, A., Fougerousse, F., Leturcq, F., Kaplan, J.C., Garcia, L. and Danos, O. (2004) Rescue of dystrophic muscle through U7 snRNA-mediated exon skipping. *Science*, **306**, 1796–1799.
30. Garcia-Gonzalo, F.R., Corbit, K.C., Sirerol-Piquer, M.S., Ramaswami, G., Otto, E.A., Noriega, T.R., Seol, A.D., Robinson, J.F., Bennett, C.L., Josifova, D.J. *et al.* (2011) A transition zone complex regulates mammalian ciliogenesis and ciliary membrane composition. *Nat. Genet.*, **43**, 776–784.
31. Plotnikova, O.V., Pugacheva, E.N. and Golemis, E.A. (2009) Primary cilia and the cell cycle. *Methods Cell. Biol.*, **94**, 137–160.
32. Garanto, A., van Beersum, S.E., Peters, T.A., Roepman, R., Cremers, F.P. and Collin, R.W. (2013) Unexpected *CEP290* mRNA Splicing in a Humanized Knock-In Mouse Model for Leber Congenital Amaurosis. *PLoS One*, **8**, e79369.
33. Vandenberghe, L.H., Bell, P., Maguire, A.M., Xiao, R., Hopkins, T.B., Grant, R., Bennett, J. and Wilson, J.M. (2013) AAV9 targets cone photoreceptors in the nonhuman primate retina. *PLoS One*, **8**, e53463.
34. Watanabe, S., Sanuki, R., Ueno, S., Koyasu, T., Hasegawa, T. and Furukawa, T. (2013) Tropisms of AAV for subretinal delivery to the neonatal mouse retina and its application for in vivo rescue of developmental photoreceptor disorders. *PLoS One*, **8**, e54146.

35. Calandrella, N., De Seta, C., Scarsella, G. and Risuleo, G. (2010) Carnitine reduces the lipoperoxidative damage of the membrane and apoptosis after induction of cell stress in experimental glaucoma. *Cell Death Dis.*, **1**, e62.
36. Rowe-Rendleman, C.L., Durazo, S.A., Kompella, U.B., Rittenhouse, K.D., Di Polo, A., Weiner, A.L., Grossniklaus, H.E., Naash, M.I., Lewin, A.S., Horsager, A. *et al.* (2014) Drug and gene delivery to the back of the eye: from bench to bedside. *Invest. Ophthalmol. Vis. Sci.*, **55**, 2714–2730.
37. Boye, S.E., Boye, S.L., Lewin, A.S. and Hauswirth, W.W. (2013) A comprehensive review of retinal gene therapy. *Mol. Ther.*, **21**, 509–519.
38. Bennett, J., Ashtari, M., Wellman, J., Marshall, K.A., Cyckowski, L.L., Chung, D.C., McCague, S., Pierce, E.A., Chen, Y., Bennicelli, J.L. *et al.* (2012) AAV2 gene therapy readministration in three adults with congenital blindness. *Sci. Transl. Med.*, **4**, 120ra115.
39. Colella, P., Trapani, I., Cesi, G., Sommella, A., Manfredi, A., Puppo, A., Iodice, C., Rossi, S., Simonelli, F., Giunti, M. *et al.* (2014) Efficient gene delivery to the cone-enriched pig retina by dual AAV vectors. *Gene Ther.*, **21**, 450–456.
40. Lopes, V.S., Boye, S.E., Louie, C.M., Boye, S., Dyka, F., Chiodo, V., Fofo, H., Hauswirth, W.W. and Williams, D.S. (2013) Retinal gene therapy with a large *MYO7A* cDNA using adeno-associated virus. *Gene Ther.*, **20**, 824–833.
41. Burnight, E.R., Wiley, L.A., Drack, A.V., Braun, T.A., Anfinson, K.R., Kaalberg, E.E., Halder, J.A., Affatigato, L.M., Mullins, R.F., Stone, E.M. *et al.* (2014) *CEP290* gene transfer rescues Leber congenital amaurosis cellular phenotype. *Gene Ther.*, **21**, 662–672.
42. Surace, E.M. and Auricchio, A. (2008) Versatility of AAV vectors for retinal gene transfer. *Vision Res.*, **48**, 353–359.
43. Cideciyan, A.V., Rachel, R.A., Aleman, T.S., Swider, M., Schwartz, S.B., Sumaroka, A., Roman, A.J., Stone, E.M., Jacobson, S.G. and Swaroop, A. (2011) Cone photoreceptors are the main targets for gene therapy of *NPHP5* (*IQCB1*) or *NPHP6* (*CEP290*) blindness: generation of an all-cone Nphp6 hypomorph mouse that mimics the human retinal ciliopathy. *Hum. Mol. Genet.*, **20**, 1411–1423.
44. Lentz, J.J., Jodelka, F.M., Hinrich, A.J., McCaffrey, K.E., Farris, H.E., Spalitta, M.J., Bazan, N.G., Duelli, D.M., Rigo, F. and Hastings, M.L. (2013) Rescue of hearing and vestibular function by antisense oligonucleotides in a mouse model of human deafness. *Nat. Med.*, **19**, 345–350.
45. Benhar, I., London, A. and Schwartz, M. (2012) The privileged immunity of immune privileged organs: the case of the eye. *Front. Immunol.*, **3**, 296.
46. Gerard, X., Perrault, I., Munnich, A., Kaplan, J. and Rozet, J.M. (2015) Intravitreal injection of Splice-switching Oligonucleotides to Manipulate Splicing in Retinal Cells. *Mol. Ther. Nucleic Acids*, **4**, e250.
47. Murray, S.F., Jazayeri, A., Matthes, M.T., Yasumura, D., Yang, H., Peralta, R., Watt, A., Freier, S., Hung, G., Adamson, P.S., *et al.* (2015) Allele-specific inhibition of Rhodopsin with an Antisense Oligonucleotide slows Photoreceptor Cell Degeneration. *Invest. Ophthalmol. Vis. Sci.*, **56**, 6362–6375.
48. Sharma, V.K., Sharma, R.K. and Singh, S.K. (2014) Antisense oligonucleotides: modifications and clinical trials. *Medchemcomm*, **5**, 1454–1471.
49. Dalkara, D., Byrne, L.C., Klimczak, R.R., Visel, M., Yin, L., Merigan, W.H., Flannery, J.G. and Schaffer, D.V. (2013) In vivo-directed evolution of a new adeno-associated virus for therapeutic outer retinal gene delivery from the vitreous. *Sci. Transl. Med.*, **5**, 189ra176.
50. Kay, C.N., Ryals, R.C., Aslanidi, G.V., Min, S.H., Ruan, Q., Sun, J., Dyka, F.M., Kasuga, D., Ayala, A.E., Van Vliet, K. *et al.* (2013) Targeting photoreceptors via intravitreal delivery using novel, capsid-mutated AAV vectors. *PLoS One*, **8**, e62097.
51. Cideciyan, A.V., Aleman, T.S., Jacobson, S.G., Khanna, H., Sumaroka, A., Aguirre, G.K., Schwartz, S.B., Windsor, E.A., He, S., Chang, B. *et al.* (2007) Centrosomal-ciliary gene *CEP290/NPHP6* mutations result in blindness with unexpected sparing of photoreceptors and visual brain: implications for therapy of Leber congenital amaurosis. *Hum. Mutat.*, **28**, 1074–1083.
52. Boye, S.E., Huang, W.C., Roman, A.J., Sumaroka, A., Boye, S.L., Ryals, R.C., Olivares, M.B., Ruan, Q., Tucker, B.A., Stone, E.M. *et al.* (2014) Natural history of cone disease in the murine model of Leber congenital amaurosis due to *CEP290* mutation: determining the timing and expectation of therapy. *PLoS One*, **9**, e92928.
53. Shafique, S., Siddiqi, S., Schraders, M., Oostrik, J., Ayub, H., Bilal, A., Ajmal, M., Seco, C.Z., Strom, T.M., Mansoor, A. *et al.* (2014) Genetic spectrum of autosomal recessive non-syndromic hearing loss in pakistani families. *PLoS One*, **9**, e100146.
54. Rasband, W.S. (1997-2012) *U. S. National Institutes of Health*. Bethesda, MD. http://imagej.nih.gov/ij/, last accessed April 25, 2016.